


First-principles study of solid hydrogen: Comparison among four exchange-correlation functionalsHuan-Cheng Yang,^{1,2} Kai Liu ^{2,3,*}, Zhong-Yi Lu,^{2,3,†} and Hai-Qing Lin¹¹*Simulation of Physical Systems Division, Beijing Computational Science Research Center, Beijing 100193, China*²*Department of Physics, Renmin University of China, Beijing 100872, China*³*Beijing Key Laboratory of Opto-electronic Functional Materials & Micro-nano Devices, Renmin University of China, Beijing 100872, China*

(Received 1 March 2020; revised 24 September 2020; accepted 30 October 2020; published 23 November 2020)

The structures of solid hydrogen under high pressures have been revisited by using first-principles electronic structure calculations. Focusing on the stability, the intramolecular bond strength of hydrogen molecules in solid hydrogen, and the cell volume, we made a comparison study on seven structures including *P21/c-24*, *C2/c-24*, *P6122-36*, *Pc-48*, *Pca21-48*, *Cmca-4*, and *Cmca-12* with the recently proposed strongly constrained and appropriately normed (SCAN) functional and three conventional exchange-correlation functionals, namely Perdew-Burke-Ernzerhof (PBE), Becke-Lee-Yang-Parr (BLYP), and van der Waals-density functional (vdW-DF). On one hand, with the SCAN functional the *C2/c* structure takes the minimum static lattice enthalpies in the pressure range from 150 to 450 GPa, which agrees with the recent synchrotron infrared spectroscopic study and is similar to the result of the BLYP functional. On the other hand, the vibration frequencies of hydrogen molecules calculated by the SCAN functional match well with the experimental characteristic IR and Raman peaks, which indicates that the SCAN functional gives a reasonable estimation of the bond strength or bond length of hydrogen molecules in solid hydrogen, while the BLYP and vdW-DF functionals overestimate the bond strength. All SCAN, PBE, BLYP, and vdW-DF functionals give a good estimation of the unit cell volumes. Thus, the structures optimized with the SCAN functional can be an excellent starting point for advanced works on solid hydrogen.

DOI: [10.1103/PhysRevB.102.174109](https://doi.org/10.1103/PhysRevB.102.174109)**I. INTRODUCTION**

Hydrogen is the most abundant element in the universe and can exist over a very large range of temperatures and pressures. Thus, determining the phase diagram and the equation of state of hydrogen is not only scientifically but also technically significant. This is relevant to many aspects, such as studying inertial confinement fusion, searching room-temperature superconductor, modeling the composition and formation of Jupiter and Saturn, and so on [1]. However, since the available experimental techniques under extreme conditions are limited, the study of hydrogen is still a relatively open subject.

Despite its atomic simplicity, the structures of dense hydrogen are surprisingly complex under extreme thermodynamic conditions, especially under high pressure. Experimentally, the diamond anvil cell (DAC) is a unique apparatus capable of generating ultrahigh static pressure of hundreds of GPa for studying hydrogen compression, and the pressure limit of current routine experiments using the DAC technology is ~ 400 GPa [2]. Up to now, the extensive experiments have characterized five phases of solid molecular hydrogen below 400 GPa and up to room temperature [3–11]. The x-ray diffraction (XRD) is a robust tool for determining the crystal structure of materials, however, it is severely hampered in

characterizing solid hydrogen due to the weak scattering of x rays by hydrogen atoms. Thus, only phase I is determined as space group *P63/mmc*, which consists of freely rotating hydrogen molecules [12,13]. Then, Raman and infrared (IR) vibrational spectroscopies have become the main tools to characterize the structures of solid hydrogen under high pressure. Although the Raman and IR data cannot provide sufficient information for determining the crystalline structure for a specific phase, they can indeed give key features to distinguish different phases under certain thermodynamic conditions. Phase II is characterized by a new additional IR peak at 45 cm^{-1} appearing below the old vibron as the pressure increases to about 110 GPa and it is suggested as a lower symmetry structure than Phase I by the orientational ordering of hydrogen molecules [14]. Phase III is discovered by the observation of a discontinuity of the Raman vibron above ~ 150 GPa at 77 K [5] and characterized by a single strong IR active vibron peak with a much larger IR vibron absorption than phase II [3,15]. Then at 300 K and above 230 GPa, phase IV is identified by two vibrons in its Raman spectrum, in which the high-frequency vibron peak is weakly dependent on pressure and the strong Raman vibron peak at lower frequency softens rapidly with applied pressure [9]. As the pressure continues to increase above 325 GPa at 300 K, phase V is discovered and characterized by the substantial weakening of vibrational Raman activity, a change in pressure dependence of the fundamental vibrational frequency and partial loss of the low-frequency excitations [11]. In addition to playing an important role in distinguishing different phases of

*kliu@ruc.edu.cn

†zlu@ruc.edu.cn

solid hydrogen experimentally, these rich and detailed Raman and IR data also provide a unique reference for theoretical research. Specifically, in the absence of XRD data, these data put an important restriction on the crystal structures of different phases of solid hydrogen.

Theoretically, a number of structures with low enthalpies have been predicted in the pressure range from 100 to 400 GPa by using density-functional-theory (DFT) based crystal structure searching tools [16]. Then these structures were checked further for determining the candidate structures of the experimentally characterized phases (phase II to phase V). Adopting the Perdew-Burke-Ernzerhof (PBE) exchange-correlation functional, Pickard and coworkers suggested a structure with $P21/c$ space-group symmetry and 24 hydrogen atoms in a unit cell (labeled as $P21/c-24$, the same below) as a candidate structure of phase II because its calculated enthalpy is slightly lower than all other known structures in the pressure range of 75 to 108 GPa [17]. The candidate structure for phase III was predicted as $C2/c-24$ or $P6122-36$ (by using the PBE and BLYP functionals), since the main features of both Raman and IR spectra calculated for these two structures are comparable to the ones observed in experiments [16,18]. With the inclusion of zero-point motion of protons and the temperature effect, the energetic and spectroscopic results show that the structures $Pc-48$ and $Pca21-48$ are promising model structures for phases IV and V, respectively [19–21]. Although the candidate structures for phase II to phase V have been suggested currently, there has always been controversy due to the complexity and subtlety of these research works because the energy differences among these structures introduced by the static enthalpies, the zero-point motion of protons, the anharmonic effects, and the errors of electronic correlation are at the same scale [20,22]. Thus, there are still many works in need to be done to solidify these results, especially the reliability of candidate structures.

Considering the irreplaceability of DFT-based electronic structure calculations for theoretically determining the candidate structures of solid hydrogen in which the exchange-correlation functional plays a decisive role, we did a comparison study on the selected exchange-correlation functionals. We performed this study based on three considerations. First, in addition to the conventionally used PBE, BLYP, and vdW-DF functionals in solid hydrogen study, we employed a new functional named strongly constrained and appropriately normed semilocal density functional (SCAN). The SCAN functional is a new semilocal functional at meta-generalized-gradient approximation (meta-GGA) level proposed by Perdew and coworkers [23]. Tests on many materials demonstrated that the SCAN functional can capture the intermediate-range van der Waals (vdW) interaction self-consistently [24], which should be considered carefully for studying solid hydrogen under high pressures [25]. Second, we studied seven typical structures $P21/c-24$, $C2/c-24$, $P6122-36$, $Pc-48$, $Pca21-48$, $Cmca-4$, and $Cmca-12$ as a whole, in which the first five are candidate structures corresponding to the experimentally indicated phase II to phase V (here both $C2/c-24$ and $P6122-36$ are candidate structures for phase III) and the remaining two were widely studied in literatures, which facilitates a comprehensive comparison. Last, we studied the internal structures in detail, especially the

intramolecular bond strength of hydrogen molecules, which are closely related to the frequencies of high-frequency IR and Raman peaks. This provides another way to examine the applicability of exchange-correlation functionals, different from the theoretically self-based benchmark [26,27].

II. METHOD

To study the structures of solid hydrogen under high pressures, we employed four kinds of exchange-correlation functionals, namely SCAN [23], PBE [28], BLYP [29,30], and vdW-DF [31]. All calculations were performed with the QUANTUM ESPRESSO (QE) package [32,33]. The norm-conserving pseudopotential generated by Yao and Kanai [34] was used for the SCAN calculations and the PAW-type pseudopotential [35,36] was used for the PBE, BLYP, and vdW-DF calculations. The kinetic energy cutoff of the plane-wave basis was set to be 1224 eV (90 Ry) for the SCAN calculations considering its additional dependence on the kinetic energy density, and to be 920 eV for the PBE, BLYP, and vdW-DF calculations. The Brillouin zone was sampled with dense Monkhorst-Pack [37] grids of approximately $0.020-0.028$ ($2\pi/\text{\AA}$). In the structure optimization, the convergence criteria for energy and force were $1 \mu\text{eV}$ and 0.01 eV/\AA , respectively. To study the phonon modes at the Brillouin zone center, the \mathbf{k} mesh was set to about 0.02 ($2\pi/\text{\AA}$) and the convergence criteria for energy and force were $0.1 \mu\text{eV}$ and 0.005 eV/\AA , respectively. The force constants were calculated with the finite displacement method for the SCAN functional [38] due to its infeasibility in the density functional perturbation theory [39], by which the force constants for the PBE, BLYP, and vdW-DF functionals were calculated.

III. RESULTS AND ANALYSIS

Many structures were proposed for solid hydrogen in the pressure range from 100 to 400 GPa. By using the first-principles electronic structure calculations based on the PBE or BLYP functionals, the candidate structures for phases II, III, IV, and V of solid hydrogen have been suggested to be $P21/c-24$, $C2/c-24$ and $P6122-36$, $Pc-48$, and $Pca21-48$, respectively [16–21]. Here, we studied these five structures together with another two widely considered structures ($Cmca-4$ and $Cmca-12$) by using the four kinds of exchange-correlation functionals.

Figure 1 shows the relative static lattice enthalpies of the $P21/c-24$, $P6122-36$, $Pc-48$, $Pca21-48$, $Cmca-4$, and $Cmca-12$ structures with respect to that of the $C2/c-24$ structure calculated with the SCAN functional. In the pressure range from 150 to 450 GPa, the $C2/c$ structure takes the minimum enthalpy, being the candidate structure of phase III, which agrees with the recent synchrotron infrared spectroscopic study by Loubeyre *et al.* [40]. In detail, the relative static lattice enthalpies of the structure $P6122$ are less than 1 meV/atom in the pressure range from 150 to 300 GPa, which is insufficient to rule out $P6122$ being a candidate structure of phase III due to the numerical precision of DFT. This agrees with the previous prediction proposing that phase III was polymorphic [18,41]. Additionally, the $P21/c-24$ structure takes the lowest enthalpy when the pressure is less than

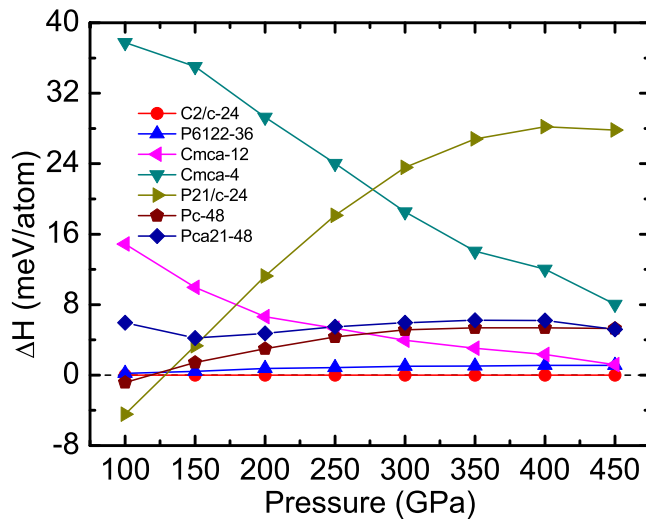


FIG. 1. The relative static lattice enthalpies of structures $P21/c-24$, $P6122-36$, $Pc-48$, $Pca21-48$, $Cmca-4$, and $Cmca-12$ with respect to structure $C2/c-24$ calculated by the SCAN functional.

125 GPa, which agrees well with the previous theoretical results that $P21/c-24$ is a candidate structure for phase II [17]. Compared with the PBE and BLYP results by Drummond *et al.* [20], the relative static lattice enthalpies calculated by the SCAN functional are similar to the BLYP results, except for a small quantitative difference, especially for the $Cmca-4$ structure. The relative static lattice enthalpies of the structures $Cmca-12$ and $Cmca-4$ calculated by the PBE functional become negative at about 275 and 330 GPa [20], respectively, implying a low metallization pressure, which is inconsistent with the experimental results [7,40]. Thus, the results of static lattice calculations using the SCAN functional can set a solid agreement between theoretical and experimental data. We will discuss the effects of proton motion later in the discussion section.

In addition to comparing the relative enthalpies among the selected structures, another important aspect for theoretically determining the structures of solid hydrogen is comparing the calculated Raman and IR spectra of the selected structures with the experimental data. Since the momentum of a photon is negligible, the Raman and IR measurements are closely related to the phonon modes at the Brillouin zone (BZ) center (here we mainly considered the first-order process). Thus, we studied the phonon frequencies at the BZ center for the structure $C2/c$ at 200 GPa. As shown in Fig. 2, we find that the main discrepancies of the phonon frequencies calculated by these four functionals are from the high-frequency part, which is closely related to the vibration of hydrogen molecules. The cyan lines denote the two characteristic experimental peaks, namely the IR peak at the higher frequency and the Raman peak at the lower frequency, respectively [7,42,43], which correspond to the two groups of vibration frequencies of hydrogen molecules. The frequencies calculated by both the SCAN and PBE functionals are in good agreement with the frequencies of the two characteristic peaks. In comparison, the frequencies calculated by both the BLYP and vdW-DF functionals miss the lower characteristic peak. We know that

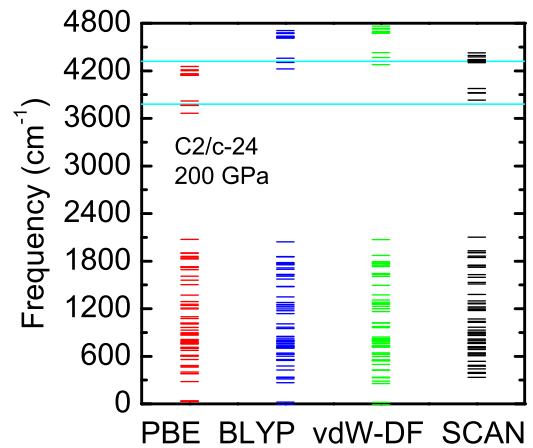


FIG. 2. The phonon frequencies at the Brillouin zone center calculated, respectively, by the SCAN, PBE, BLYP, and vdW-DF functionals for structure $C2/c-24$ at 200 GPa. The cyan lines at the higher and lower frequencies denote the experimental IR and Raman peaks, respectively, from Refs. [7,42,43].

although the symmetry of the structures determines the numbers of IR and Raman modes, their frequencies are closely related to the inner details of each structure, for example, the high-frequency part is determined by the intramolecular bond strength or bond length in some sense.

As shown in Fig. 3, the bond lengths of hydrogen molecules for structure $C2/c$ are classified into two categories, which lead to two groups of vibration frequencies shown in Fig. 2. The bond lengths calculated by the SCAN functional are between those calculated by the PBE and vdW-DF(BLYP) functionals. Based on the analysis on data from Figs. 2 and 3, both the BLYP and vdW-DF functionals overestimate the bond strength or underestimate the bond lengths, which agrees with the quantum Monte Carlo calculation (QMC) results that the vdW-DF functional overestimates the curvature of the molecular potential at the equilibrium bond

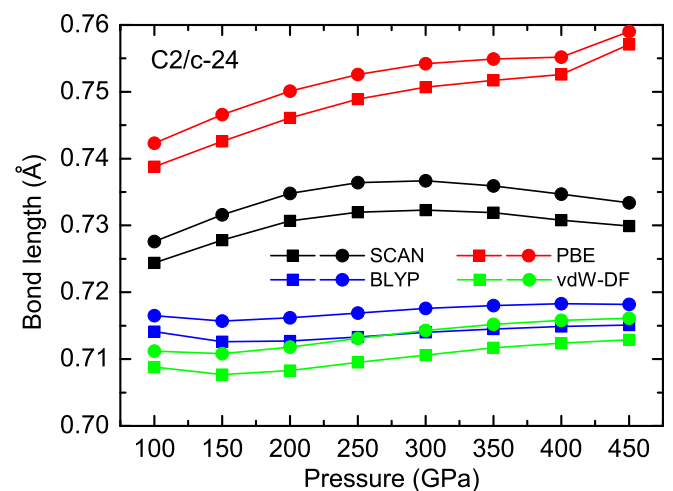


FIG. 3. The bond lengths of hydrogen molecules for structure $C2/c-24$ calculated, respectively, by the SCAN, PBE, BLYP, and vdW-DF functionals.

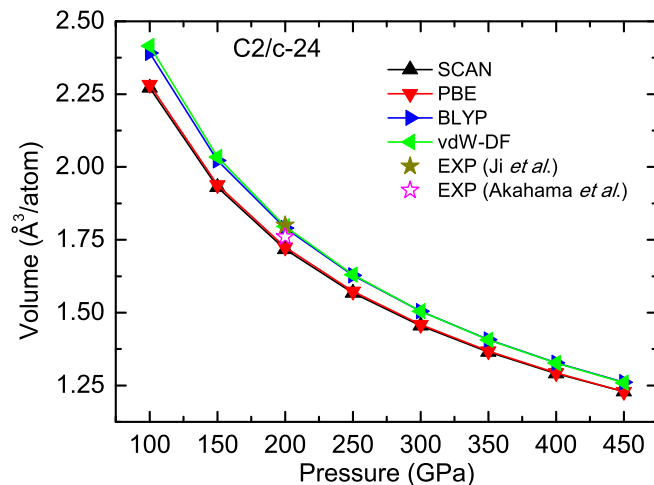


FIG. 4. The average volumes per hydrogen atom for structures $C2/c-24$ calculated, respectively, by the SCAN, PBE, BLYP, and vdW-DF functionals. The two experimental values are from Refs. [45,46].

length under high pressure (yielding a shorter bond length by 1%) [26,44]. Specifically, the two experimental characteristic peaks locate at the upper limits of the two groups of vibration frequencies calculated by the PBE functional, respectively, while they locate at the lower limits of those calculated by the SCAN functional, respectively (Fig. 2). Moreover, the benchmark work based on the QMC calculations also showed that the PBE functional underestimates the bond strength (yielding a longer bond length by about 5%) [26,44]. Therefore, combining our data and the data from literatures, we conclude that the SCAN functional gives a reasonable estimation of the bond strength or bond lengths of hydrogen molecules.

In the study of solid hydrogen, the unit cell volume under different pressures is also an important physical quantity that needs to be determined. Figure 4 shows the average volumes per hydrogen atom for the structure $C2/c$ calculated by these four functionals. The cell volumes calculated by the SCAN and PBE functionals are very similar (difference within 1%), and the case for BLYP and vdW-DF functionals is the same (difference also within 1%). In the pressure range from 100 to 450 GPa, the cell volumes calculated by the SCAN functional are about 5.8%–2.5% smaller than those by the BLYP

functional and the corresponding difference decreases with increasing pressures. In Fig. 4, we also show two experimental data points at 200 GPa, one is extracted from the XRD results at 300 K up to 254 GPa by Ji *et al.* [45], the other is extrapolated from the XRD results at 100 K up to 190 GPa by Akahama *et al.* [46]. At 200 GPa, the cell volume calculated by the SCAN functional is about 4.5% and 2.4% smaller than those by Ji *et al.* and Akahama *et al.*, respectively. Considering that the experimental values are measured at finite temperature (with thermal expansion) and the calculated values are just static lattice results at 0 K (without thermal expansion), the cell volumes calculated by the SCAN functional are reasonable, and it is so with the PBE functional. On the other hand, the cell volumes calculated by both BLYP and vdW-DF functionals at 0 K coincide with the experimental value at the room temperature by Ji *et al.* Moreover, our calculations also show that under all studied pressures the differences of cell volumes among these seven structures are small (within 1.5%), as shown in Table I. Conclusively, all SCAN, PBE, BLYP, and vdW-DF functionals yield good estimation of the average volumes per hydrogen atom.

IV. DISCUSSION

Regarding the contribution of proton motion at high pressure and low temperature, the harmonic zero-point energy, which can be obtained by normal phonon calculations, plays an important role. Taking the relative harmonic zero-point energy calculated with the PBE functional by Drummond *et al.* as a reference [20], we analyze the influence of proton motion on the stability of these structures. With the inclusion of the PBE's harmonic zero-point energies into our SCAN's static lattice results, the $C2/c-24$ structure takes the minimum total enthalpies from about 150 GPa up to about 380 GPa among the structures $P21/c-24$, $C2/c-24$, $Pc-48$, $Cmca-4$, and $Cmca-12$, while the $Cmca-12$ structure takes the minimum total enthalpies above 380 GPa. Additionally, according to the results from Ref. [18], the $P6122-36$ structure takes a negative relative zero-point energy, larger than 1 meV/atom, with respect to $C2/c-24$ structure from 150 to 200 GPa. By adding these zero-point energies to the static lattice enthalpies calculated by the SCAN functional, we find that the total enthalpies of $P6122-36$ structure may be smaller (within 1 meV/atom) than those of $C2/c-24$ structure from about 150 GPa up to about 230 GPa. Thus, with the inclusion of the har-

TABLE I. The average volumes per hydrogen atom for structures $P21/c-24$, $C2/c-24$, $P6122-36$, $Pc-48$, $Pca21-48$, $Cmca-4$, and $Cmca-12$ calculated by the SCAN functionals at different pressures. The errors represent the maximum deviation of these structures with respect to their average.

Pressure (GPa)	$P21/c$	$C2/c$	$P6122$	Pc	$Pca21$	$Cmca-4$	$Cmca-12$	Error
100	2.2950	2.2716	2.2732	2.2814	2.2609	2.2603	2.2523	1.07%
150	1.9580	1.9306	1.9316	1.9359	1.9301	1.9055	1.9171	1.46%
200	1.7417	1.7173	1.7178	1.7221	1.7199	1.6963	1.7093	1.39%
250	1.5869	1.5677	1.5681	1.5710	1.5691	1.5495	1.5626	1.21%
300	1.4680	1.4545	1.4550	1.4651	1.4599	1.4373	1.4504	1.15%
350	1.3716	1.3648	1.3653	1.3652	1.3656	1.3498	1.3613	1.00%
400	1.2918	1.2909	1.2913	1.2909	1.2898	1.2768	1.2869	0.90%
450	1.2218	1.2285	1.2278	1.2281	1.2249	1.2165	1.2240	0.65%

monic zero-point energies, in the pressure range from 150 to 380 GPa, the $P6122-36$ structure takes the minimum total enthalpies below ~ 230 GPa and then the $C2/c-24$ structure takes the minimum total enthalpies. Overall, the conclusion drawn from the static lattice results by the SCAN functional can hold well qualitatively. On the other hand, with the inclusion of the harmonic zero-point energies [20,21] into our SCAN static lattice enthalpies of the candidate structure $Pc-48$ for phase IV and the candidate structure $Pca21-48$ for phase V, the total enthalpies of these two structures are both larger than those of the $C2/c-24$ structure above 250 GPa, which agrees with the experimental findings that phases IV and V were not discovered at low temperature [7,40] but discovered at 300 K above 230 GPa [9] and at 300 K above 325 GPa [11], respectively. Therefore, for the aspect of relative stability, the SCAN functional can give a reasonable estimation.

The recent room-temperature single-crystal x-ray diffraction study on solid hydrogen up to 254 GPa has demonstrated that the high-pressure transitions in solid hydrogen are not caused by major crystallographic changes and the mass centers of hydrogen molecules for both phases III and IV remain in the hexagonal close packed (hcp) configuration as phase I [45]. Inspired by this study, we examine the aforementioned seven structures by calculating the mass-center coordinates of hydrogen molecules and checking the symmetry of the mass centers. We find that with a coarse tolerance of 0.35 Å, the mass centers of the five candidate structures ($P21/c-24$, $C2/c-24$, $P6122-36$, $Pc-48$, and $Pca21-48$) for phase II to phase V are all at $P63/mmc$ sites under all pressures (except the Pc structure at 150, 200, and 250 GPa). In contrast, the mass centers of the other two widely studied noncandidate structures $Cmca-4$ and $Cmca-12$ are at $Im-3m$ sites with tolerance of 0.2 and 0.4 Å, respectively. In addition, we find that the bond lengths and orientations of hydrogen molecules vary from structure to structure. Overall, the above results indicate that these five candidate structures ($P21/c-24$, $C2/c-24$, $P6122-36$, $Pc-48$, and $Pca21-48$) can be considered as deformations of the $P63/mmc$ structure by changing the bond lengths and the orientations of hydrogen molecules together with small mass center deviations. This agrees well with the experimental statement that the high-pressure transitions in solid hydrogen are molecular-symmetry-breaking isostructural transition of hydrogen molecules [45]. Considering that phase I is determined experimentally as the $P63/mmc$ structure, which

consists of freely rotating molecules and can be thought as a series of structures with the same energy and mass centers but with various orientations of hydrogen molecules, we speculate that as pressure increases the degeneracy is lifted and the anisotropy increases, eventually leading to the emergence of experimentally indicated phase II to phase V. Thus, we can search new candidate structures of solid hydrogen based on such initial structures, in which the mass centers of hydrogen molecules locate at the hcp sites.

V. CONCLUSION

We have done a comparison study by using four exchange-correlation functionals (SCAN, PBE, BLYP, and vdW-DF) on seven structures of solid hydrogen under high pressure: $P21/c-24$, $C2/c-24$, $P6122-36$, $Pc-48$, $Pca21-48$, $Cmca-4$, and $Cmca-12$, respectively. The first five structures are the proposed candidate structures for phase II to phase V and the remaining two structures are also widely considered. We find that the SCAN functional gives an overall appropriate estimation of all three aspects that we focus, namely energetics, bond strength or lengths, and cell volumes. Thus, the structures determined by the SCAN functional can be an excellent starting point for advanced works on solid hydrogen to deal with more complex effects, such as many-body correlations. The mass center symmetry of the five candidate structures are all $P63/mmc$ with a coarse tolerance, which hints a clue or provides a constraint to predict new candidate structures for solid hydrogen.

ACKNOWLEDGMENTS

We thank Cheng Ji for helpful discussions. This work was supported by the Joint Fund of National Natural Science Foundation of China and China Academy of Engineering Physics (NSAF) (Grant No. U1930402), the Science Challenging Program (Grant No. TZ2016001), the National Key R&D Program of China (Grants No. 2017YFA0302903 and No. 2019YFA0308603), and the National Natural Science Foundation of China (Grants No. 11774422 and No. 11774424). Computational resources were provided by the Beijing Computational Science Research Centre and the Physical Laboratory of High Performance Computing at Renmin University of China.

-
- [1] J. M. McMahon, M. A. Morales, C. Pierleoni, and D. M. Ceperley, *Rev. Mod. Phys.* **84**, 1607 (2012).
 - [2] H. K. Mao, X. J. Chen, Y. Ding, B. Li, and L. Wang, *Rev. Mod. Phys.* **90**, 015007 (2018).
 - [3] H. K. Mao and R. J. Hemley, *Rev. Mod. Phys.* **66**, 671 (1994).
 - [4] H. E. Lorenzana, I. F. Silvera, and K. A. Goettel, *Phys. Rev. Lett.* **64**, 1939 (1990).
 - [5] R. J. Hemley and H. K. Mao, *Phys. Rev. Lett.* **61**, 857 (1988).
 - [6] H. E. Lorenzana, I. F. Silvera, and K. A. Goettel, *Phys. Rev. Lett.* **63**, 2080 (1989).
 - [7] C. S. Zha, Z. X. Liu, and R. J. Hemley, *Phys. Rev. Lett.* **108**, 146402 (2012).
 - [8] M. I. Eremets and I. A. Troyan, *Nat. Mater.* **10**, 927 (2011).
 - [9] R. T. Howie, C. L. Guillaume, T. Scheler, A. F. Goncharov, and E. Gregoryanz, *Phys. Rev. Lett.* **108**, 125501 (2012).
 - [10] C. S. Zha, R. E. Cohen, H. K. Mao, and R. J. Hemley, *Proc. Natl. Acad. Sci.* **111**, 4792 (2014).
 - [11] P. D. Simpson, R. T. Howie, and E. Gregoryanz, *Nature (London)* **529**, 63 (2016).
 - [12] P. Loubeyre, R. LeToullec, D. Hausermann, M. Hanfland, R. J. Hemley, H. K. Mao, and L. W. Finger, *Nature* **383**, 702 (1996).

- [13] H. K. Mao, A. P. Jephcoat, R. J. Hemley, L. W. Finger, C. S. Zha, R. M. Hazen, and D. E. Cox, *Science* **239**, 1131 (1988).
- [14] M. Hanfland, R. J. Hemley, and H. K. Mao, *Phys. Rev. Lett.* **70**, 3760 (1993).
- [15] R. J. Hemley, Z. G. Soos, M. Hanfland, and H. K. Mao, *Nature* **369**, 384 (1994).
- [16] C. J. Pickard and R. J. Needs, *Nat. Phys.* **3**, 473 (2007).
- [17] C. J. Pickard and R. J. Needs, *Phys. Status Solidi B* **246**, 536 (2009).
- [18] B. Monserrat, R. J. Needs, E. Gregoryanz, and C. J. Pickard, *Phys. Rev. B* **94**, 134101 (2016).
- [19] C. J. Pickard, M. Martinez-Canales, and R. J. Needs, *Phys. Rev. B* **85**, 214114 (2012).
- [20] N. D. Drummond, B. Monserrat, J. H. L. Williams, P. L. Ríos, C. J. Pickard, and R. J. Needs, *Nat. Commun.* **6**, 7794 (2015).
- [21] B. Monserrat, N. D. Drummond, P. Dalladay-Simpson, R. T. Howie, P. L. Lopez Ríos, E. Gregoryanz, C. J. Pickard, and R. J. Needs, *Phys. Rev. Lett.* **120**, 255701 (2018).
- [22] S. Azadi and W. M. C. Foulkes, *Phys. Rev. B* **88**, 014115 (2013).
- [23] J. W. Sun, A. Ruzsinszky, and J. P. Perdew, *Phys. Rev. Lett.* **115**, 036402 (2015).
- [24] J. W. Sun, R. C. Remsing, Y. B. Zhang, Z. R. Sun, A. Ruzsinszky, H. W. Peng, Z. H. Yang, A. Paul, U. Waghmare, X. F. Wu, M. L. Klein, and J. P. Perdew, *Nat. Chem.* **8**, 831 (2016).
- [25] S. Azadi and G. J. Ackland, *Phys. Chem. Chem. Phys.* **19**, 21829 (2017).
- [26] R. C. Clay, III, J. McMinis, J. M. McMahon, C. Pierleoni, D. M. Ceperley, and M. A. Morales, *Phys. Rev. B* **89**, 184106 (2014).
- [27] K. Liao, X.-Z. Li, A. Alavi, and A. Grüneis, *NPJ Comput. Mater.* **5**, 110 (2019).
- [28] J. P. Perdew, K. Burke, and M. Ernzerhof, *Phys. Rev. Lett.* **77**, 3865 (1996).
- [29] A. D. Becke, *Phys. Rev. A* **38**, 3098 (1988).
- [30] C. Lee, W. Yang, and R. G. Parr, *Phys. Rev. B* **37**, 785 (1988).
- [31] M. Dion, H. Rydberg, E. Schröder, D. C. Langreth, and B. I. Lundqvist, *Phys. Rev. Lett.* **92**, 246401 (2004).
- [32] P. Giannozzi *et al.*, *J. Phys.: Condens. Matter* **21**, 395502 (2009).
- [33] P. Giannozzi *et al.*, *J. Phys.: Condens. Matter* **29**, 465901 (2017).
- [34] Y. Yao and Y. Kanai, *J. Chem. Phys.* **146**, 224105 (2017).
- [35] P. E. Blöchl, *Phys. Rev. B* **50**, 17953 (1994).
- [36] G. Kresse and D. Joubert, *Phys. Rev. B* **59**, 1758 (1999).
- [37] H. J. Monkhorst and J. D. Pack, *Phys. Rev. B* **13**, 5188 (1976).
- [38] K. Parlinski, Z. Q. Li, and Y. Kawazoe, *Phys. Rev. Lett.* **78**, 4063 (1997).
- [39] S. Baroni, S. de Gironcoli, A. Dal Corso, and P. Giannozzi, *Rev. Mod. Phys.* **73**, 515 (2001).
- [40] P. Loubeyre, F. Occelli, and P. Dumas, *Nature* **577**, 631 (2020).
- [41] S. Azadi and T. D. Kühne, *Phys. Rev. B* **100**, 155103 (2019).
- [42] A. F. Goncharov, E. Gregoryanz, R. J. Hemley, and H. K. Mao, *Proc. Natl. Acad. Sci.* **98**, 14234 (2001).
- [43] P. Loubeyre, F. Occelli, and R. LeToullec, *Nature* **416**, 613 (2002).
- [44] J. McMinis, R. C. Clay III, D. Lee and M. A. Morales, *Phys. Rev. Lett.* **114**, 105305 (2015).
- [45] C. Ji, B. Li, W. J. Liu, J. S. Smith, A. Majumdar, W. Luo, R. Ahuja, J. F. Shu, J. Y. Wang, S. Sinogeikin, Y. Meng, V. B. Prakapenka, E. Greenberg, R. Q. Xu, X. R. Huang, W. G. Yang, G. Y. Shen, W. L. Mao, and H. K. Mao, *Nature* **573**, 558 (2019).
- [46] Y. Akahama, Y. Mizuki, S. Nakano, N. Hirao, and Y. Ohishi, *J. Phys. Conf. Ser.* **950**, 042060 (2017).